Ecological Modelling 386 (2018) 1–10

Contents lists available at ScienceDirect

Ecological Modelling

journal homepage: www.elsevier.com/locate/ecolmodel

# Fine-scale analysis of urban flooding reduction from green infrastructure: An ecosystem services approach for the management of water flows

Denis Maragno[a], Mattias Gaglio[b,*], Martina Robbi[a], Federica Appiotti[a], Elisa Anna Fano[b], Elena Gissi[a]

[a] Department of Planning and Design in Complex Environment, IUAV University of Venice, S. Croce 1957, 30135 Venice, Italy
[b] Department of Life Sciences and Biotechnology, University of Ferrara, Via L. Borsari 46, 44121 Ferrara, Italy

ARTICLE INFO

*Keywords:*
Remote sensing
Ecosystem service supply
Ecosystem service demand
Runoff control
Urban green spaces
Flood vulnerability index

ABSTRACT

Climate change is expected to modify the timing and amount of precipitation in the future, increasing the demand for effective adaptation at the local scale, especially to mitigate the impacts of extreme events, expected to increase in frequency and magnitude. Green infrastructure (GI) can provide a crucial water regulating ecosystem service, helping communities to adapt to the increased stormwater runoff and associated flood risks expected from climate change. This paper presents a new planning tool that utilizes remote sensing and census data to model the supply and demand for urban flood reduction services through GI. A high-resolution urban digital model is used to distinguish between permeable and impermeable areas at fine (e.g. 25 cm) spatial scale. Flood reduction capacity was modeled using two indices: i) the amount of runoff reduced by existing GI, and ii) the runoff reduction coefficient. We also analyzed the flood reduction demand using a vulnerability index. The tool is demonstrated in a historical urban center of the Northern Italy, with different scenarios used to identify priority areas of intervention. The results show that the flood reduction capacity is unevenly distributed throughout the study area. Public and private surfaces contribute different amounts of runoff with different flood reduction potentials. In eight of nine urban study areas, private properties generate more runoff than public properties under the worst scenario conditions. The study identified two priority areas of intervention, based on their mismatch between supply and demand of GI's water regulating services.

## 1. Introduction

Because of the proliferation of impervious surfaces, urban regions are extremely vulnerable to the effects of climate change on precipitation, and less resilient than rural settlements to a wide range of climate-related disturbances (Ashley et al., 2005; Huong and Pathirana, 2013). Climatic change is expected to exacerbate precipitation patterns in future (Schröter et al., 2005), increasing the demand for a suite of water-related services (Zheng et al., 2016).

Because the impacts of climate change are experienced locally (Carter et al., 2015), many cities are developing mitigation and adaptation strategies to reduce their vulnerability (Musco et al., 2016; Rangarajan et al., 2015; Rosenzweig et al., 2011; Zidar et al., 2017a). Effective local adaptation strategies are needed specifically to mitigate the consequences of extreme events, which are predicted to increase in frequency and magnitude (IPCC, 2014) in the years to come.

A paradigm shift is needed, to replace the outdated resistance-based approach (e.g. requiring the construction of new hard infrastructure) with an ecosystem-based approach (Ojea, 2015) that seeks to restore, enhance, or create ecosystem services within the urban matrix. The latter would promote the conservation and restoration of natural systems specifically for the benefits they provide to humans, e.g. ecosystem services (ES) (Temmerman et al., 2013).

Green infrastructure (GI) has been defined as 'all natural, semi-natural and artificial networks of multifunctional ecological systems within, around, and between urban areas, at all spatial scales' (Tzoulas et al., 2007). This definition includes a wide range of ecosystem types, which provide many different bundles of ES. Among these, several regulating services are particularly relevant in urban contexts including climate regulation, air quality regulation, water flow regulation, water purification (Haase et al., 2014).

Water regulation refers to the control of surface water flows so as to maintain normal levels in the watershed (De Groot et al., 2002). In the urban context, water regulation often refers to the control of stormwater runoff and associated flooding (Gómez-Baggethun et al., 2010; McPhearson et al., 2014), which can cause severe damage to public and

* Corresponding author.
*E-mail address:* gglmts@unife.it (M. Gaglio).

https://doi.org/10.1016/j.ecolmodel.2018.08.002
Received 2 February 2018; Received in revised form 13 July 2018; Accepted 1 August 2018
Available online 13 August 2018

private assets and negatively impact the quality of life and human safety (Hammond et al., 2015). Because it was typically designed to convey historical "design storms", conventional urban drainage infrastructure is often ineffective at managing runoff during the extreme events attributed to climate change (Ashley et al., 2005). In this context, GI is gaining increased attention by both researchers and urban planners (de Sousa et al., 2016a,b, 2012; Haase et al., 2014; Mason and Montalto, 2014; Rangarajan et al., 2015) because it can be used to retrofit water regulating services into urban landscapes that are currently inadequately serviced by existing drainage systems. The approach is often synergistic with other municipal efforts to restore ecosystems heavily impacted by previous and ongoing phases of urbanization (Haaland and van den Bosch, 2015).

An increasing number of studies have described the ES that can potentially be delivered by urban GI (Endreny et al., 2017; Pappalardo et al., 2017; Pulighe et al., 2016; Wang et al., 2014) but very few tools have been put forth to enable their incorporation in urban decision-making processes (e.g. Kabisch, 2015; Nikodinoska et al., 2018). A joint analysis of ES supply and demand could be used to inform decision-making processes around ES delivery (Burkhard et al., 2012; Gissi and Garramone, 2018). The supply of ES is defined as the capacity of a particular planning area or ecosystem to provide ES (Burkhard et al., 2012), while the demand for ES is defined as those ES that are recognized or desired by beneficiaries or end users in the study area (Wolff et al., 2015).

Such an approach would help to transfer the ES concept from theory to practice, one of the most important contemporary challenges in ES science (Gissi et al., 2015; Gissi and Garramone, 2018). Though different methods for mapping ES provision capacity (i.e. ecological functions) are presented in literature, e.g. direct measures, proxy indicators and models (Egoh et al., 2012), rarely are these combined in a contextual analysis of ES demand (Wolff et al., 2015). Once recent exception is Zidar et al. (2017b) who used a map of seven ecosystem service gaps, e.g. geographic regions no longer capable of providing the ES most needed by the residents of Camden, New Jersey, as a planning tool for siting and designing multifunctional GI.

Assessment of ES demand differs according the purpose of the analysis. In another context, the targets fixed by energy plans can be used to quantify the demand for bioenergy provision by incorporating ES trade-off analysis (Gissi et al., 2018, 2016). Wolff et al. (2015) classify demand types in four typologies: risk reduction, preferences and values, direct use or consumption of goods and services. Among these, the need for risk reduction can be used for assess demand of flood mitigation (Liquete et al., 2013; Nedkov and Burkhard, 2012).

By identifying priority areas for ES management and protection, ES can be incorporated into a wide range of local efforts to adapt to climate change. For example, Snäll et al. (2016) demonstrated that spatial conservation prioritization could represent a suitable tool for GI design, allowing cost-effective allocation of conservation efforts. Verhagen et al. (2017) mapped capacity and demand for five ES at European level. They found that ignoring ES demand led to the siting of interventions in remote regions where the ES benefits to society were small.

This paper presents a new planning tool that utilizes remote sensing and census data to model the supply and demand for urban flood reduction services through GI. The study focuses on flood reduction ES provided by GI, defined as the capacity of urban GI to absorb urban stormwater to reduce the risk of flooding. We define urban GI as all the pervious green spaces within the urban study area, on both private and public properties. First, we introduce the method for mapping the supply of flood reduction services from existing urban GI. A high-resolution urban digital model was used to distinguish between permeable and impermeable areas at fine scale, with a precision of 25 cm. Next, we classified the pervious areas based on their soils, vegetation, construction materials, and land cover coverage, utilizing the SCS (Soil Conservation Service) Curve Number (CN) method (USDA - Soil Conservation Service, 1972) to quantify runoff generation at the catchment scale. Regions generating more runoff are assumed to generate greater flood risk. Because the analysis is carried out at the catchment, and not the watershed scale, watershed slopes are ignored. Flood reduction capacity is evaluated using two indices: i) the amount of runoff reduced by green spaces (Δv) (Zhang et al., 2012), and ii) the runoff reduction coefficient (Cr). Secondly, we analyzed the demand for flooding reduction through the computation of a Vulnerability Index (VI), which represents the vulnerability of local population and buildings to urban flooding. The method was applied to the historical urban center of Dolo, a highly urbanized area in Northern Italy. The analysis was replicated for 24 scenarios of rain events, emerging from the combination of three factors: i) precipitation depth, ii) antecedent moisture condition of soils and iii) conditions of initial abstraction. Finally, we matched the flooding reduction capacity of urban GI with the respective demand for such service, in order to identify priority areas of intervention where to urgently mitigate potential flooding events.

## 2. Methods

### 2.1. Study area

The study area comprises the historical urban center of the Municipality of Dolo (coordinates 45°25′29.57″N 12°04′32.92″E), located inside the Metropolitan Area of Venice, Italy. The municipality of Dolo covers 24.8 $km^2$ and has a total population of approximately 15,000 inhabitants, of which 4226 live inside the historical urban center (1.67 $km^2$). It is located within the watershed of the Venice lagoon.

The climate of the study area is classified as B1 (Humid) according to the Thornthwaite classification (Feddema, 2005), with an average temperature is 13.2 °C. Mean rainfall ranges from 600 and 1100 mm $yr^{-1}$, with an annual average of 912 mm. The mean annual reference evapotranspiration is 730 mm (Aschonitis et al., 2017). Historically, the wettest month is May (94.4 mm), while the driest is January (49.9 mm). The hydraulic soil group of this area is classified as B type according to the USDA-NRCS classification (NRCS, 1986). Soils belonging to this category typically have between 10% and 20% clay and 50% to 90% sand with a loamy sand or sandy loam texture (USDA, 2009).

The historical urban center of Dolo is frequently subjected to urban flooding events because of an inadequately sized urban drainage system and large amount of impervious surfaces (Municipality of Dolo, 2012). Evidence of the effects of climate change has been detected and studied by Bixio (2009). A 60-year analysis (1956–2010) of precipitation patterns in the Venice lagoon drainage basin (where Dolo is situated) reveals an intensification of events rainfall accompanied by simultaneous reduction in annual precipitation totals. In September 2007, several high-intensity, short duration rainfall events generated runoff in excess of the conveyance capacity of the local drainage infrastructure, generating extreme flood damage (Municipality of Dolo, 2012).

### 2.2. High-resolution urban digital model

A high-resolution urban digital model of all of the pervious and impervious elements, both public and private, within the historical urban center of Dolo and their relative heights was generated from a variety of data sets. Soil maps were generated by processing spatial data obtained from LIDAR (Light Detention and Ranging) survey using ArcGis 10.3 (ESRI). An aerial survey commissioned by the Metropolitan City of Venice Administration in 2014 produced 4000 high-resolution images. Then, a 3D digital model of the area was created with the Dense Image Matching technique (Hirschmüller, 2008). Raster images -DSM (Digital Surface Model) and DTM (Digital Terrain Model) were generated with a precision of 25 cm (Pixel 0.25 m). The DSM reports the altimetric data of all natural and anthropogenic elements (namely impervious) in a specific area, while the DTM reports the morphology of

**Table 1**
Ground cover classes and respective Curve Number (CN) values.

| Ground cover class | Description | CN | References |
|---|---|---|---|
| Gravel | | 85 | Hawkins et al. (2009) |
| Semipermeable blocks | | 97 | Hawkins et al. (2009) |
| Concrete | | 98 | Hawkins et al. (2009) |
| Asphalt | | 98 | Hawkins et al. (2009) |
| Rubberway pervious pavement | | 97 | Shirini and Imaninasab (2016) |
| Other impervious | | 98 | Hawkins et al. (2009) |
| Bare soil | | 86 | Hawkins et al. (2009) |
| Agricultural land | as Straight row at poor condition | 81 | Hawkins et al. (2009) |
| Short vegetation | | 61 | Hawkins et al. (2009) |
| Open space with tall vegetation | as Open space at poor condition (grass cover > 50%) | 79 | Hawkins et al. (2009) |
| Water | | 0 | Hawkins et al. (2009) |

the territory without anthropogenic elements and vegetation (Maragno et al., 2015). Finally, a digital atlas was created to distinguish between permeable and impermeable areas in grid squares of 25 × 25 cm. The Atlas also reports the elevation of each element, allowing the three-dimensional volumes of all natural (e.g. bushes and trees) and anthropogenic (e.g. buildings) elements to be computed.

### 2.3. GI and ground coverage classification

Since the remote sensing surveys provided three dimensional datasets, the urban vegetation could have classified according to the height: tall vegetation (> 1.5 m) and short vegetation (< 1.5 m). A field survey was performed in order to improve the digital atlas and correct bias due to the presence of ornamental plants in terraces or roofs. The areas classified as tall vegetation (i.e. urban trees) were detailed depending on the ground coverage beneath them. This correction was necessary because soil physical properties are determinant factors affecting urban flooding and runoff (Holman-Dodds et al., 2003). The impervious surfaces were further classified by the material type for their capacity to retain water and promote infiltration through field survey. Descriptions for each ground coverage type are presented in Table 1.

The analysis was carried out at both the lot and section scales. Firstly, the study area was classified in private and public properties. Subsequently, private properties were subdivided into lots using polygons drawn around individual property units. Public areas were subdivided into zone destinations, using the procedures of Panduro and Veie (2013). Urban sections boundaries were derived from the Italian National Institute of Statistic (ISTAT) and represent the minimum territorial units inside municipalities where census records are collected.

### 2.4. Runoff calculation

The generation of urban runoff was modeled using the SCS Curve Number (CN) method (USDA - Soil Conservation Service, 1972). This model estimates rainfall runoff (i.e. urban flooding generated by rainfall) based on ground coverage, soil type and precipitation. The model calculation is computed on three parameters (precipitation depth, initial abstraction and potential maximum storage of soil) and it is based on the following equations:

$$Q = \begin{cases} (P-I_a)^2/(P-I_a+S), & P \geq I_a \\ 0, & P \leq I_a \end{cases} \quad (1)$$

$$S = \frac{25400}{CN} - 254 \quad (2)$$

$$I_a = \lambda \bullet S \quad (3)$$

Where Q is the rainfall runoff depth (mm), P is the precipitation depth (mm), S is the potential maximum water storage in soil (mm), CN is the tabulated value of Curve Number (dimensionless) ranging from 0 to 100, $I_a$ is the initial abstraction of rainfall (mm) and λ is the initial abstraction coefficient (constant).

The CN values were derived from (Hawkins et al., 2009), and mainly depends on corresponding soil coverage type (described in Section 2.3), Hydrological Soil Group (HSG) and Antecedent Moisture Condition (AMC). The higher is the CN value the higher is the runoff generated by a ground surface in a rain event.

The contribution of urban pervious and impervious areas to runoff generation and reduction was calculated at both property and urban section levels. At the property level, the overall CN for each unit was calculated as weighted average of values for respective areas, as follow:

$$CN_p = \frac{\sum_i CN_i \bullet A_i}{\sum_i A_i} \quad (4)$$

Where the $CN_p$ is the weighted curve number of the property *p*, $CN_i$ and Ai are the curve number and the area of the *i* soil coverage type, respectively.

At urban section level, the total runoff depth was computed considering the values of each polygon:

$$Q_s = \frac{\sum Q_p \bullet A_p}{A_s} \quad (5)$$

Where $Q_s$ and $Q_p$ are the runoff depth (mm) and $A_s$ and $A_p$ are the areas of the *s* urban section and of *p* property, respectively.

### 2.5. Mapping runoff (flooding) reduction capacity

In order to estimate the contribution of each spatial unit to runoff reduction, two indexes were calculated: the amount of runoff reduced by green spaces (Δv) in $m^3$ (Zhang et al., 2012) and the runoff reduction coefficient (Cr) (Yao et al., 2015). These indexes express the reduction of surface runoff provided by the presence of urban green spaces and pervious surfaces and therefore are proposed in this analysis as a proxy for the capacity to deliver the ES of urban flood reduction. Δv quantifies the general benefit provided by green spaces, in terms of runoff volume reduction, calculated as follow:

$$\Delta_v = \sum_i 0.001 \bullet (Q_b - Q_i) \bullet A_i \quad (6)$$

Where Δv is the runoff reduction ($m^3$), $Q_b$ is the runoff depth (mm) generated by a hypothetical scenario in which all existing green spaces are replaced by 100% impervious surfaces (CN = 98), $Q_i$ is the runoff depth (mm) generated by the spatial unit given its actual configuration of green spaces and $A_i$ is the area of each spatial unit inside the computation area.

Cr represent the efficiency in runoff reduction. The index was calculated as follow:

$$C_r = \Delta_v \bullet (0.001 \bullet P \bullet A)^{-1} \quad (7)$$

Where Cr is runoff reduction coefficient (adimensional, ranging between 0 and 1), Δv is the runoff reduction ($m^3$), P is the daily rainfall

**Table 2**
The four precipitation depths considered for scenario simulations.

| Precipitation depth (mm) | Description | Frequency | Source |
|---|---|---|---|
| 10 | Mean daily value (per hour) | 69 per year | ARPAV |
| 45 | High daily value (per hour) | 32 per year | ARPAV |
| 90 | Capacity limit of the urban drainage network (on 3 h) | 20 years | Municipal Water Plan (Municipality of Dolo, 2012) |
| 168 | Extreme event (16/09/2009) (per hour) | unknown | ARPAV |

depth (mm) and A the area ($m^2$) of each urban section. This index expresses the capacity of pervious surfaces of each area (i.e. section) to avoid flooding events and, therefore, can be considered as an indicator for this ES.

A higher Δv means greater potential hydrologic benefits provided by existing urban green space, whereas a higher Cr indicates less need to improve future urban water flow management in a specific urban section.

### 2.6. Scenario analysis

The flood reduction capacity was evaluated for different scenarios, which simulate the potential conditions of rainfall and flood generation depending on three factors: i) rainfall depth ($P_i$) (four precipitation values); ii) the Antecedent Moisture Condition (AMC), and iii) the $I_a$ values. The four precipitation depths considered in the analysis were 10, 45, 90 and 160 mm (Table 2). These values were chosen according to their relevance on planning decisions. In fact, the 10 mm and 45 mm precipitation depths correspond to the mean and high average daily values, respectively. A three-hourly precipitation depth of 90 mm was calculated by the Municipal Water Plan (Municipality of Dolo, 2012) as the capacity threshold of the urban drainage network. Finally, the daily rainfall depth of 160 mm was the most extreme event recorded (2009) by the Regional Agency for Environmental Protection (ARPAV).

NRCS classifies three AMC classes, representing the relative moisture before the rainfall event: “dry” (AMC-I), “moderate/normal” (AMC-II) and “wet” (AMC-III) conditions. Since soil absorption capacity is lower in wet soils, CN values attributed to a specific soil coverage with a specific HSG should be corrected for the antecedent conditions (CN for AMC-III > AMC-II > AMC-I).

The initial abstraction coefficient (λ) is usually defined equal to 0.2 (USDA - Soil Conservation Service, 1972). However, some studies proposed different values, particularly for urban areas (Lim et al., 2006; Ling and Yusop, 2014). Therefore, we built the scenarios considering two values of $I_a$, 0.2 and 0.05, accordingly.

The analysis of Δv and Cr was performed for the 24 scenarios deriving from the combination of the three factors ($P_i$, AMC, $I_a$).

### 2.7. Assessing flooding reduction demand

Since the flow of ESs is defined as the intersection between the supply capacity (described in this study by the Eq. (7)) and the demand (Burkhard et al., 2012), the latter is fundamental to inform urban planning. The demand for the flood reduction service was calculated as a function of people and buildings vulnerability (Derkzen et al., 2017):

$$VI_i = X_{1i} + X_{2i} + ..X_{ni} \quad (8)$$

Where $VI_i$ is Vulnerability Index of the i section, $X_{ni}$ are the single vulnerability for each of the n parameter (adjusted for 0 to 1) of the i section describing local population and buildings vulnerability (see Supplementary materials). The index is based on the expectation that some population (e.g. children, elderly people and foreigners) and building categories (e.g. buildings with poor or bad status conditions) are more susceptible to the consequences of urban flooding. All the parameters computed in Eq. (9) are assumed to have the same importance (i.e. weight). The VI was calculated per each urban section with the statistical data from the National census (source: ISTAT).

### 2.8. Priority areas of intervention

In order to orient urban planning to implement mitigation actions, a ranking of the priority areas of intervention (i.e. section ranking) was provided, through a Priority Index (PRI), as follows:

$$PRI = \frac{(VI + 1)\bullet(Q_s + 1)}{Cr} \quad (9)$$

Where VI is the Vulnerability Index, $Q_s$ is the generated runoff depth (mm) and Cr is the Reduction Coefficient under the hypothesis of the most pessimistic scenario (i.e. AMC-III and Ia = 0.05). All the parameters were calculated at urban section level.

We assume that: i) the lower is the Cr (ES supply) the higher is the potential benefit that could be reached by the inclusion of new GI in the related urban section, ii) the higher are the vulnerability of local population and buildings (ES demand) and the urban runoff (Q) the higher is priority for intervention. Hence, the priority of intervention will be attributed to urban sections where: i) the mismatch between ES demand and supply is higher, and ii) the runoff is larger.

## 3. Results

### 3.1. Spatial analysis of green infrastructures

The spatial analysis reveals that GI is unevenly distributed in the historical urban center of Dolo, and that the existing GI is fragmented and scattered (Fig.1). Pervious areas cover 43.6% of the total study area. Small patches of tall vegetation mainly characterize the pervious areas within Dolo urban center, except for an urban park at the east side of the study area with tallest vegetation (up to 29 m). Table 3 shows the ground cover distribution for the study area, subdivided into public and private properties.

### 3.2. Flooding reduction supply capacity

Fig. 2 shows the spatial distribution of the runoff depth generated under the 24 different scenarios, considering the combinations of AMC, $I_a$ and precipitations. The results at section levels are presented in Table 4. The relative contributions of public and private areas to the total runoff roughly follow those of the respective total areas.

The capacity of urban green spaces to mitigate runoff (e.g. Cr values) under different values of AMC and $I_a$ are shown in Fig. 3. Public and private surfaces contribute differently to the total runoff and showed different performances of flooding reduction. In eight urban sections out of nine, private properties generate more runoff than public ones under the worst scenario conditions (Table 4). The same trend can be observed also for runoff depth and for Cr (i.e. the contribution of GI to reduce rainfall runoff), with higher ES performances for public areas than private proprieties.

Since Cr depends on precipitation, as well as on soil conditions and initial abstractions, the index was modeled under a rainfall gradient for the different AMC and $I_a$ values (Fig. 4a, b). This analysis allows identifying the optimal precipitation value to which the ES provision capacity of the study area is maximum. The maximum Cr values range within 0.345 and 0.389 (observed at the rainfall values of 13 and 103 mm, respectively), according to the different combinations of biophysical factors.


**Fig. 1.** Ground cover and vegetation height of the study area (a) and urban section boundaries (b) of the study area.

### 3.3. Flooding reduction demand

The vulnerability indices (VI) for all the urban sections of the municipality of Dolo are shown in Fig. 5a and Table 5. The highest VI values were computed for no. 5, which lies in the northeastern part of the study area. This ranking is due principally to population and, to a lesser extent, buildings conditions. The center population is densely inhabited by more vulnerable categories of people, such as children and elderly. The sections with a higher demand of the flooding reduction service are those with the larger percentages of public properties (sections 5 and 9) (Table 5).

### 3.4. Priority rank of intervention

Table 5 shows the PRI values calculated for the four rainfall depths considered in the scenarios, considering with AMC-III and $I_a = 0.05$. Fig. 5b shows the PRI computed considering runoff and Cr at the rainfall depth of 90 mm, corresponding to the critical threshold for drainage network according to the Municipality Water Plan (Municipality of Dolo, 2012), with AMC-III and $I_a = 0.05$. These values for Antecedent Moisture Condition and initial abstraction were chosen for the priority rank calculation according a conservative approach. In fact, they represent the worst possible conditions for runoff mitigation. The values for PRI, as well as for the single components (VI, runoff and Cr), are shown in Table 5. According to the results, the urgency of interventions for improving the green infrastructures in the study area should be focused on sections 8 and 3. These sections show higher values of generated runoff and the lower for Cr. Despite section 5 has the highest VI value, its low ranking is due to a good level of Cr performed, meaning that even though this area is vulnerable, the urban green spaces can mitigate flooding events. Sections 1 and 7 are those with the lower ranking score, meaning lowest priority of intervention.

## 4. Discussion

The study proposes a new methodology to incorporate a consideration of the runoff capture/flood mitigation capacity of urban GI into urban climate change planning. The model spatially analyses the supply and demand of water regulation ES, in an attempt to fill the gap between ES theory and practice in urban areas, specifically with respect to flooding.

The analysis of ES provision capacity maps the potential of urban GI to mitigate urban flooding problems associated with runoff. The Cr and runoff depth values were combined with vulnerability index to obtain the priority rank of intervention (PRI) for urban sections. The results clearly show several urban priority areas. Sections 8 and 3 are those with higher PRI values. High PRI scores for these sections are due to the lowest Cr and high runoff values, rather than to high levels of vulnerability. This means that interventions in these zones should be aimed to increase the extension and quality of green spaces. Lower PRI scores were obtained for sections 1 and 7. Section 1 showed a lower level of vulnerability and a higher performance of Cr, suggesting that the conservation of current level of ES may be obtained by the maintenance of current GI. In section 7, a lower priority was mainly due to the lower

**Table 3**
Ground coverage of the study area. Distribution of public and private properties are specified for each ground cover class.

| | Public areas | | Private areas | | Total area | |
|---|---|---|---|---|---|---|
| | $m^2$ | % | $m^2$ | % | $m^2$ | % |
| Gravel | 33172.6 | 5.39% | 34,199.4 | 3.27% | 67,371.9 | 4.05% |
| Semipermeable blocks | 13689.5 | 2.22% | 34,215.8 | 3.27% | 47,905.4 | 2.88% |
| Rubberway pervious pavement | 2477.9 | 0.40% | 0.0 | 0.00% | 2477.9 | 0.15% |
| Concrete | 50876.7 | 8.27% | 70,171.7 | 6.71% | 121,048.4 | 7.28% |
| Asphalt | 78434.0 | 12.74% | 24,791.1 | 2.37% | 103,225.1 | 6.21% |
| Bare soil | 12283.7 | 2.00% | 108,248.3 | 10.35% | 120,532.1 | 7.25% |
| Agricultural land | 0.0 | 0.00% | 1741.7 | 0.17% | 1741.7 | 0.10% |
| Open space with tall vegetation | 52470.2 | 8.53% | 160,629.6 | 15.35% | 213,099.8 | 12.82% |
| Water | 32,706.8 | 5.31% | 0.0 | 0.00% | 32,706.8 | 1.97% |
| Other impervious | 11880.7 | 1.93% | 1930.4 | 0.18% | 13,811.2 | 0.83% |
| Build-up | 81419.1 | 13.23% | 287,476.7 | 27.48% | 368,895.9 | 22.20% |
| Short vegetation | 246067.2 | 39.98% | 322,749.4 | 30.85% | 568,816.5 | 34.23% |
| Total | 615478.5 | 100% | 1,046,154.1 | 100% | 1,661,632.6 | 100% |

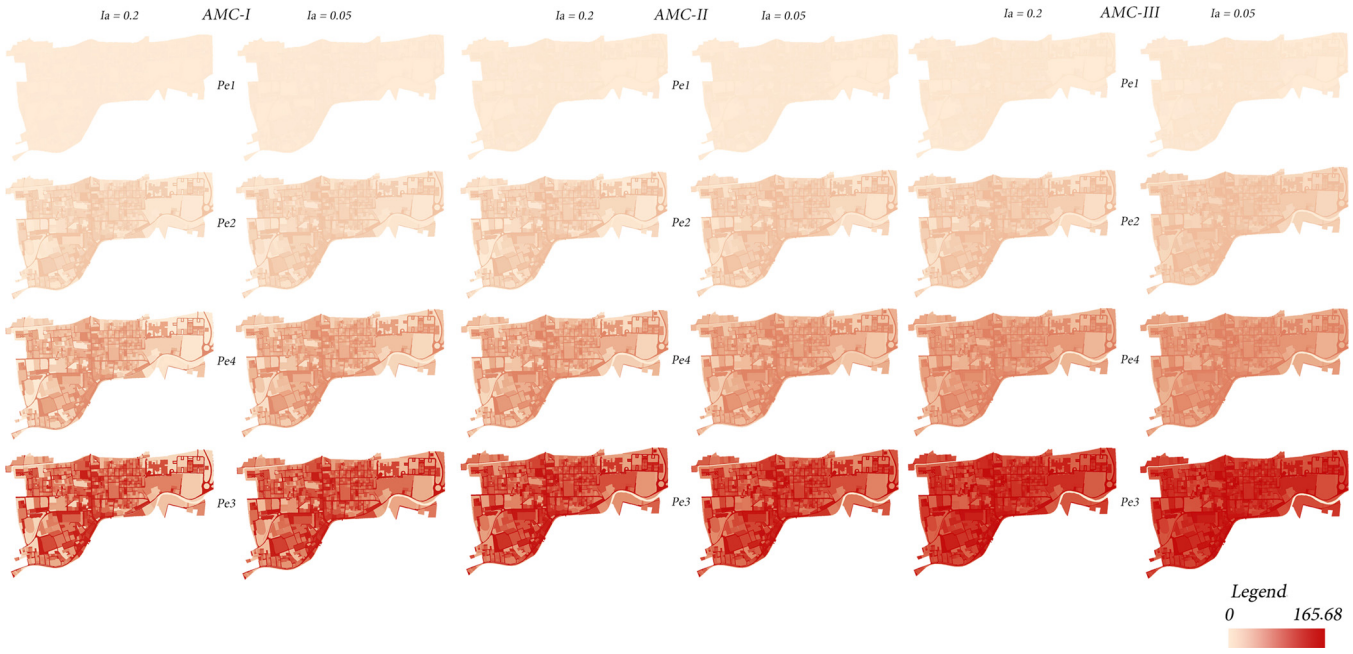


**Fig. 2.** Modelled runoff (mm) for each of the 24 considered scenarios.

runoff values. Specific attention should be payed to section 5, observed as the most vulnerable. In fact, even though the analysis did not highlight high priority of intervention for this section, the higher observed level of vulnerability suggests monitoring this area with particularly attention in case of intense rainfall events.

Since the higher runoff amount is generated by private surfaces, an incentive-based mechanism for private owners may be effective in promoting the increase of green spaces and pervious surfaces in the study area in general and in urban areas more prone to runoff generation. For example, the Biotope Area Factor (BAF) (Bauen and Becker, 1990) is an urban greening policy tools designed to improve the ecosystem's functionality and improve the development of biotopes in city centers. Measures can be applied also to public areas to improve their contribution to urban runoff mitigation. The installation of rain gardens is demonstrated to increase water infiltration and absorption by collecting water from parking, roofs and other pervious surfaces (Davis et al., 2009).

The increase and maintenance of green spaces would also lead to multiple benefits provided by urban vegetation, as air depuration from chemical and particulate pollution (Grote et al., 2016), microclimate regulation by mitigating heat waves (Gillner et al., 2015), carbon storage (Fares et al., 2017) and amelioration of urban landscape aesthetic (Southon et al., 2017). In addition, efforts for increasing people awareness to the role of green infrastructures to support human well-being may be effective to orient citizens' choices in their private proprieties.

Due to the extreme heterogeneity of build-up areas, high-resolution data are needed to capture different components of urban green spaces at fine scale (Maragno, 2016), such as urban vegetation of trees, grass and bushes, which are providers of different ecological functions (Davies et al., 2011; Jim and Chen, 2008). The use of LIDAR-derived information allowed the mapping of vegetation structure at fine scale. When these data are modeled and integrated with information concerning local ES demand, the analysis can inform urban planning by prioritizing measures and actions at urban section scale where flooding reduction is more urgently needed, as resulting from the ES demand and supply analyses.

In general, the use of remote sensing technics to map ESs is a key challenge for the ES science (Dawson et al., 2016). Many studies process images derived by passive sensors (e.g. satellite scenes) to obtain land cover maps of vegetation indexes, used to model ES in space and time (De Araujo Barbosa et al., 2015). The use of products derived by the use of active sensors (Lefsky et al., 2002), such as LIDAR, allows the access of three-dimensional information on vegetation and, for this reason, has

**Table 4**
Areas, runoff depth (mm) and volume ($m^3$) and Cr (adimensional between 0 and 1) for each urban section. Contributions of public (Pub) and private areas (Prv) are also specified. Cr is calculated for the more pessimistic scenario (i.e. AMCIII and Ia = 0.05) for the rainfall depth = 90 mm (corresponding to the critical threshold for drainage network).

| | Area | | | Runoff depth | | | Runoff volume | | | Cr | | |
|---|---|---|---|---|---|---|---|---|---|---|---|---|
| Section n° | Pub (%) | Prv (%) | Tot ($m^2$) | Pub (mm) | Prv (mm) | Tot (mm) | Pub (%) | Prv (%) | Tot ($m^3$) | Pub | Prv | Tot |
| 1 | 50.9% | 49.1% | 275,976.2 | 57.78 | 64.58 | 61.12 | 48.1% | 51.9% | 16,868.1 | 0.27 | 0.19 | 0.23 |
| 2 | 23.7% | 76.3% | 128,358.1 | 63.11 | 74.73 | 71.98 | 20.8% | 79.2% | 9238.7 | 0.20 | 0.14 | 0.16 |
| 3 | 20.2% | 79.8% | 116,444.5 | 59.91 | 72.86 | 70.24 | 17.2% | 82.8% | 8179.1 | 0.15 | 0.08 | 0.10 |
| 4 | 14.2% | 85.8% | 84,137.8 | 68.39 | 70.97 | 70.61 | 13.7% | 86.3% | 5940.7 | 0.15 | 0.10 | 0.11 |
| 5 | 44.1% | 55.9% | 138,182.3 | 64.48 | 66.72 | 65.73 | 43.2% | 56.8% | 9083.1 | 0.19 | 0.17 | 0.18 |
| 6 | 21.5% | 78.5% | 89,968.7 | 72.25 | 70.10 | 70.56 | 22.1% | 77.9% | 6348.1 | 0.13 | 0.12 | 0.12 |
| 7 | 25.0% | 75.0% | 433,922.8 | 52.96 | 61.99 | 59.73 | 22.2% | 77.8% | 25,919.5 | 0.20 | 0.13 | 0.15 |
| 8 | 31.4% | 68.6% | 85,285.1 | 59.83 | 76.96 | 71.58 | 26.3% | 73.7% | 6104.6 | 0.07 | 0.06 | 0.06 |
| 9 | 62.6% | 37.4% | 309,357.0 | 67.03 | 68.44 | 67.54 | 62.1% | 37.9% | 20,894.9 | 0.11 | 0.12 | 0.12 |

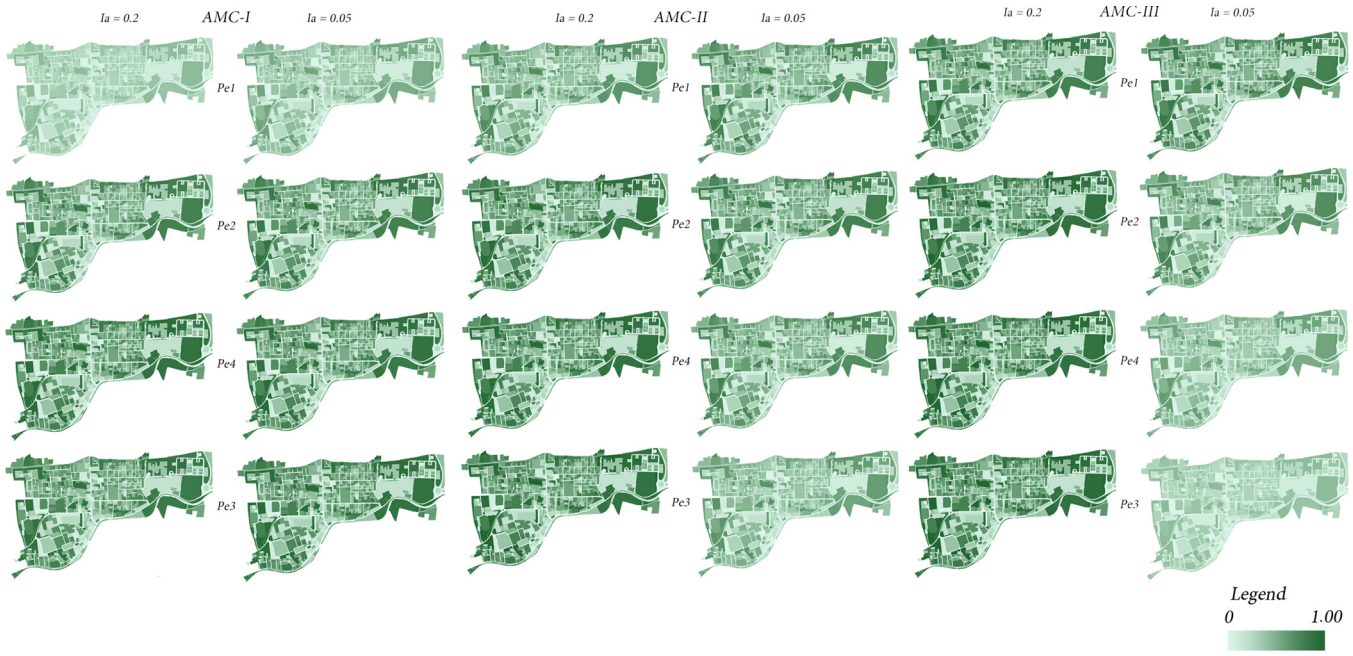


**Fig. 3.** Coefficient of Reduction (Cr) for each of the 24 considered scenarios.

greater potential in mapping vegetation structure at finer scale. Detecting spatial variation of vegetation structure is fundamental for mapping ESs in urban ecosystems (Lehmann et al., 2014). In this study, information on vegetation height was used to discriminate areas covered by tall vegetation from grass and bushes (grouped as "short vegetation"). However, field surveys were necessary to avoid erroneous interpretations for tall vegetation, due, for example, by the presence of single trees growing on small flowerbeds surrounded by impervious surfaces, rather than by permeable soil (e.g. grass).

Some limitations related to the SCS method for runoff modelling should be considered. For example, specific values for CN and initial abstraction should be calibrated on measured data in the study area to obtain reliable results. Since no empirical data were available for the study area, the uncertainties related to the AMC and $I_a$ parameters were managed by combining all the possible values in the 24 scenarios, to obtain a final range of values. AMC varies according to the previous climatic conditions and can be adjusted to describe the moisture conditions according to Ward and Trimble (2004). Furthermore, values for initial abstraction ($I_a$) can differ largely as well. The Soil Conservation Service defines Ia equal to 0.02. Nonetheless, some studies highlighted that this value could not be reliable when applied to urban landscapes (Lim et al., 2006). Ling and Yusop (2014) showed that the most adopted value for this parameter in urban contexts is 0.05. Because of the above-mentioned uncertainties, the analysis was performed accounting a set of the combinations of AMC (AMC-I-II-III) and $I_a$ values (0.02 and 0.005).

Additional limitations concern the intrinsic simplification of the model. For instance, slope and pipes and other hydraulic features were not considered. Hydrological behavior of impervious surfaces is complex to predict, as preferential runoff paths are the result of interactions with drainage systems, as well as presence of temporary and permanent barriers (Fletcher et al., 2013). In this study, the SCS model was applied on the urban historical center of Dolo, which represents only a portion of the urban catchment area. In this case, the runoff depends only on the excess of rainfall in the area, and not to the contribution of rainfall coming from other areas of the catchment as for Dolo. The model did not consider the interaction among areas (i.e., among proprieties), as well as among urban sections. The approach is focused on the individual contribution of each area in order to understand potential priority areas of intervention to control and manage the total water

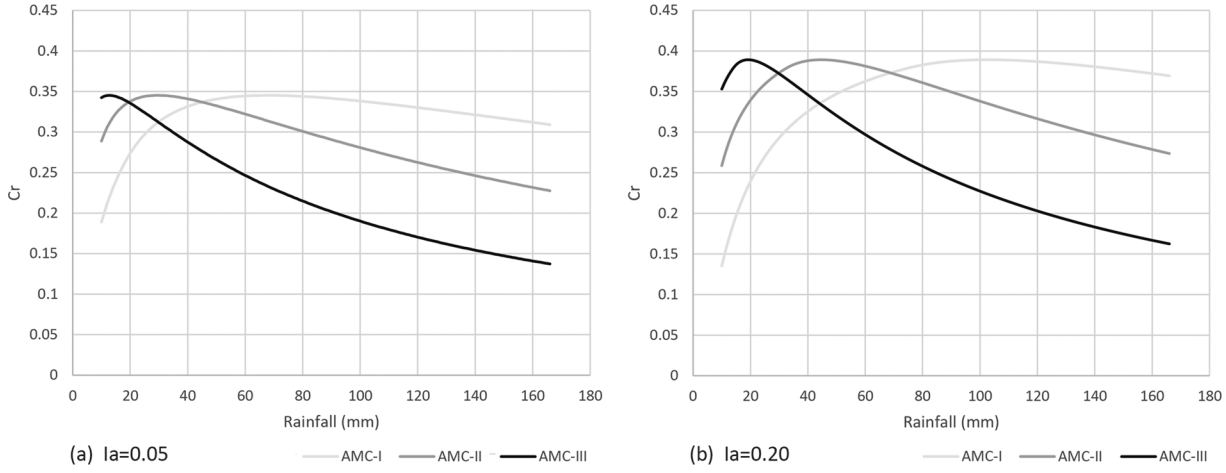


**Fig. 4.** Variation of the Coefficient of Reduction (Cr) along a rainfall gradient for the different values of AMC and with $I_a$ = 0.2 (a) and $I_a$ = 0.05 (b).

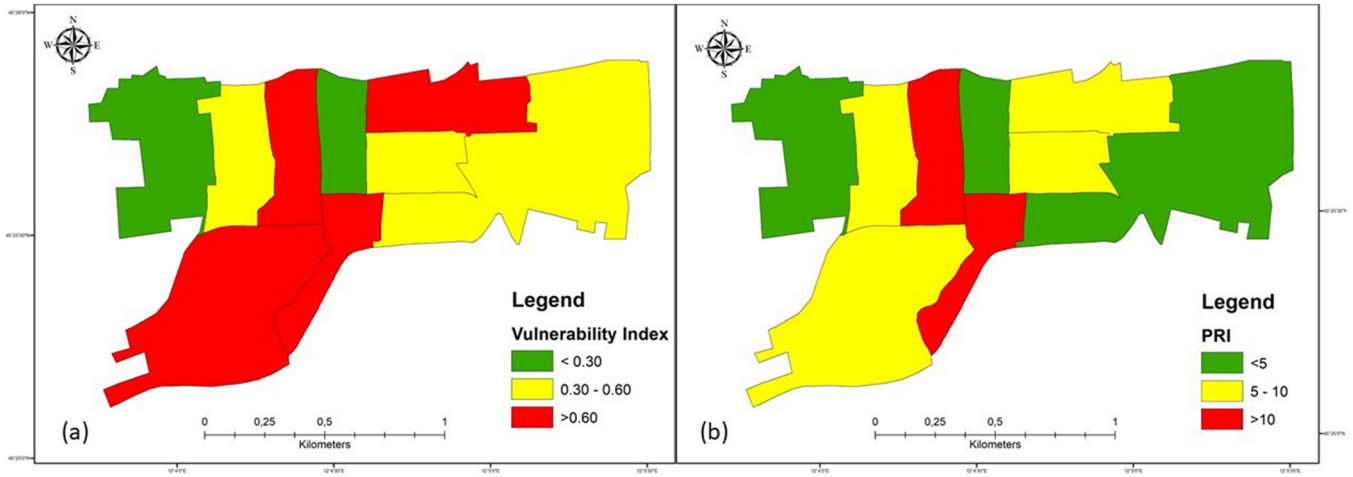


**Fig. 5.** Vulnerability Index (VI) (a) and Priority Index (PRI) (b) values obtained for each urban section.

flows in the urban area. Moreover, urban soils are difficult to be studied and sampled, because they are usually severely disturbed and show highly variable infiltration rates (Pitt et al., 1999). Our method overcomes the difficulties in sampling disturbed urban soils by considering pervious and impervious surface, which influence runoff formation (Yang et al., 2015). In any case, the output of the proposed method provides a qualitative ranking of the different zones (i.e. urban sections) for priority of intervention, rather than a quantitative assessment for drainage infrastructure calculation. Moreover, the use of normalized values, as in the case of PRI computation, can mitigate the bias due to the use of indirect measures in ES studies (e.g. Gaglio et al., 2017).

The elaboration of the results obtained from the analysis performed at private property scale leads to issues related to the use and publication of data concerning private properties. For this reason, the outcomes of this analysis should be strictly managed by public bodies under protocols dealing with confidentiality and privacy regulation, in order to guarantee the correct use as well as the privacy of citizens' data.

It has to be mentioned that the PRI considers all the parameters as equally important (see Eq. (9)). However, the index can be corrected according stakeholder perception and/or local conditions through attributing different weight at the single component.

Finally, the Cr response along a rainfall gradient was studied under the different combinations of AMC and $I_a$ (Fig. 4a and b). Since climate change are expected to increase the frequency and the magnitude of rainfall extreme events, the response of Cr along a precipitation gradient can be used to project the response of runoff mitigation service to future climate change. Fig. 4a and b suggest that the capacity of green infrastructures of the study area to regulate extreme events will decrease as a consequence of climate change. In fact, Cr values tend to decrease together with the increase of rainfall depth.

The effects of AMC seem more sensible to the rainfall variation, while those due to $I_a$ values are more relevant for determining the maximum value of Cr. For this reason, direct measures of both soil condition and initial abstraction are important for the accuracy of runoff mitigation. Maximum Cr values correspond to the breaking point of the curve, after which the Cr performance declines (Fig. 4a and b). The saturation of water retention capacity of urban green spaces during severe rainfall events and the consequent release of the excess surface water more quickly mainly causes this decrease (Yao et al., 2015). Information on the rainfall depths corresponding to the maximum Cr values represent the threshold, over which the ES declines. These thresholds may be used to activate specific early-warning measures to protect the most vulnerable population from flooding.

The different performances of rainwater retention capacity under the three different soil moisture conditions suggest that ES provision depends on the climatic conditions occurring before the extreme event. Practically, urban planning decisions should carefully consider precipitation pattern variations within the context of climate change, in order to improve adaptation strategies.

## 5. Conclusions

Climate change forces decision-makers to adaptation governance measures to mitigate risks related to the increased frequency of extreme events. Transferring ES assessment from theory to practice has great potential to support and inform such decisions, especially in urban areas. The development of tools that integrate ES supply and demand is a key challenge for the future planning and management of the most vulnerable areas, such urban ecosystems. This study elaborated a

**Table 5**
Normalized values (between 0 and 1) of Vulnerability Index (VI), runoff depth and Cr calculated for each urban section, under the more pessimistic scenario (i.e. AMC-III and Ia = 0.05) for the different precipitation values, and respective Priority Index (PRI) values (in bold).

| | | P = 10 mm | | | P = 45 mm | | | P = 168 mm | | | P = 90 mm | | |
|---|---|---|---|---|---|---|---|---|---|---|---|---|---|
| Section n° | VI | Runoff | Cr | PRI | Runoff | Cr | PRI | Runoff | Cr | PRI | Runoff | Cr | PRI |
| 1 | 0.00 | 0.12 | 0.39 | **0.00** | 0.15 | 0.31 | **0.00** | 0.13 | 0.16 | **0.00** | 0.11 | 0.23 | **0.00** |
| 2 | 0.46 | 0.58 | 0.27 | **2.75** | 0.00 | 0.21 | **2.16** | 1.00 | 0.11 | **8.78** | 1.00 | 0.16 | **5.93** |
| 3 | 0.64 | 0.77 | 0.17 | **6.83** | 0.80 | 0.13 | **8.59** | 0.69 | 0.07 | **16.37** | 0.86 | 0.10 | **12.16** |
| 4 | 0.24 | 0.78 | 0.18 | **2.43** | 0.83 | 0.14 | **3.11** | 0.69 | 0.07 | **5.83** | 0.89 | 0.11 | **4.38** |
| 5 | 1.00 | 0.45 | 0.30 | **4.77** | 0.48 | 0.25 | **6.05** | 0.41 | 0.12 | **11.68** | 0.49 | 0.18 | **8.32** |
| 6 | 0.49 | 0.73 | 0.21 | **3.98** | 0.80 | 0.17 | **5.13** | 0.75 | 0.08 | **10.13** | 0.88 | 0.12 | **7.38** |
| 7 | 0.41 | 0.00 | 0.26 | **1.61** | 0.07 | 0.21 | **2.14** | 0.00 | 0.10 | **4.04** | 0.00 | 0.15 | **2.73** |
| 8 | 0.61 | 1.00 | 0.11 | **11.11** | 1.00 | 0.09 | **13.76** | 0.60 | 0.04 | **22.40** | 0.97 | 0.06 | **18.55** |
| 9 | 0.69 | 0.52 | 0.20 | **5.37** | 0.61 | 0.16 | **7.05** | 0.50 | 0.08 | **13.36** | 0.64 | 0.12 | **9.83** |

method for the identification of priority areas of intervention for the management of urban green infrastructures, which could be applied even without the availability of runoff field measurements. The qualitative approach can assist in the identification of cost-effective measures to prioritize the need for GI management in different zones. The analysis also provides the estimation of ES demand under climate change. The projected increase of precipitation intensity is likely to overcome the GI capacities to mitigate rainfall runoff. Information on ES responses to climate change are fundamental to inform environmental managers towards more sustainable governance.

Remote sensing techniques have a great potential in supporting ES supply mapping in urban centers, by providing high-resolution maps and information that are fundamental in heterogeneous and complex ecosystems as urban areas.

## Acknowledgments

We thank the two anonyms reviewers for their suitable comments and F. Montalto for the support in revising the manuscript.

## Appendix A. Supplementary data

Supplementary material related to this article can be found, in the online version, at doi:https://doi.org/10.1016/j.ecolmodel.2018.08.002.

## References

Aschonitis, V.G., Papamichail, D., Demertzi, K., Colombani, N., Mastrocicco, M., Ghirardini, A., Castaldelli, G., Fano, E.A., 2017. High-resolution global grids of revised Priestley-Taylor and Hargreaves-Samani coefficients for assessing ASCE-standardized reference crop evapotranspiration and solar radiation. Earth Syst. Sci. Data 9, 615–638. https://doi.org/10.5194/essd-9-615-2017.

Ashley, R.M., Balmfort, D.J., Saul, A.J., Blanskby, J.D., 2005. Flooding in the future – predicting climate change, risks and responses in urban areas. Water Sci. Technol. 52, 265–273.

Landschaft Planen & Bauen, Becker Giseke Mohren Richard, 1990. The Biotope Area Factor as an Ecological Parameter. Excerpt 24.

Bixio, V., 2009. Caratteri fisici e climatici dei comprensori di bonifica del veneto. Venezia. .

Burkhard, B., Kroll, F., Nedkov, S., Müller, F., 2012. Mapping ecosystem service supply, demand and budgets. Ecol. Indic. 21, 17–29. https://doi.org/10.1016/j.ecolind.2011.06.019.

Carter, J.G., Cavan, G., Connelly, A., Guy, S., Handley, J., Kazmierczak, A., 2015. Climate change and the city: building capacity for urban adaptation. Prog. Plann. 95, 1–66. https://doi.org/10.1016/j.progress.2013.08.001.

Davies, Z.G., Edmondson, J.L., Heinemeyer, A., Leake, J.R., Gaston, K.J., 2011. Mapping an urban ecosystem service: quantifying above-ground carbon storage at a city-wide scale. J. Appl. Ecol. 48, 1125–1134. https://doi.org/10.1111/j.1365-2664.2011.02021.x.

Davis, A.P., Hunt, W.F., Traver, R.G., Clar, M., 2009. Bioretention technology: overview of current practice and future needs. J. Environ. Eng. 135, 109–117. https://doi.org/10.1061/(ASCE)0733-9372(2009)135:3(109).

Dawson, T.P., Cutler, M.E.J., Brown, C., 2016. The role of remote sensing in the development of SMART indicators for ecosystem services assessment. Biodiversity 17, 136–148. https://doi.org/10.1080/14888386.2016.1246384.

De Araujo Barbosa, C.C., Atkinson, P.M., Dearing, J.A., 2015. Remote sensing of ecosystem services: a systematic review. Ecol. Indic. 52, 430–443. https://doi.org/10.1016/j.ecolind.2015.01.007.

De Groot, R.S., Wilson, M.A., Boumans, R.M.J., 2002. A typology for the classification, description and valuation of ecosystem functions, goods and services. Ecol. Econ. 41, 393–408. https://doi.org/10.1016/S0921-8009(02)00089-7.

de Sousa, M.R.C., Montalto, F.A., Spatari, S., 2012. Using life cycle assessment to evaluate green and grey combined sewer overflow control strategies. J. Ind. Ecol. 16, 901–913. https://doi.org/10.1111/j.1530-9290.2012.00534.x.

de Sousa, M.R.C., Montalto, F.A., Gurian, P., 2016a. Evaluating green infrastructure stormwater capture performance under extreme precipitation. J. Extreme Events 3 (2). https://doi.org/10.1142/S2345737616500068. 1650006-1-1650006-24.

de Sousa, M.R.C., Montalto, F.A., Palmer, M.I., 2016b. Potential climate change impacts on green infrastructure vegetation. Urban For. Urban Green. 20, 128–139. https://doi.org/10.1016/j.ufug.2016.08.014.

Derkzen, M.L., van Teeffelen, A.J.A., Verburg, P.H., 2017. Green infrastructure for urban climate adaptation: how do residents' views on climate impacts and green infrastructure shape adaptation preferences? Landsc. Urban Plann. 157, 106–130. https://doi.org/10.1016/j.landurbplan.2016.05.027.

Egoh, B., Drakou, E.G., Dunbar, M.B., Maes, J., Willemen, L., 2012. Indicators for mapping ecosystem services: a review. JRC Scientific and Policy Reports.

Endreny, T., Santagata, R., Perna, A., Stefano, C., De Rallo, R.F., Ulgiati, S., 2017. Implementing and managing urban forests: a much needed conservation strategy to increase ecosystem services and urban wellbeing. Ecol. Modell. 360, 328–335. https://doi.org/10.1016/j.ecolmodel.2017.07.016.

Fares, S., Paoletti, E., Calfapietra, C., Mikkelsen, T.N., Samson, R., Le Thiec, D., 2017. Carbon sequestration by urban trees. In: In: Pearlmutter, D., Calfapietra, C., Samson, R., O'Brien, L., Ostoić, S.K., Sanesi, G., del Amo, R.A. (Eds.), The Urban Forest: Cultivating Green Infrastructure for People and the Environment Vol. 7. Springer International Publishing, pp. 31–39. https://doi.org/10.1007/978-3-319-50280-9_4.

Feddema, J.J., 2005. A revised thornthwaite-type global climate classification. Phys. Geogr. 26, 442–466. https://doi.org/10.2747/0272-3646.26.6.442.

Fletcher, T.D., Andrieu, H., Hamel, P., 2013. Understanding, management and modelling of urban hydrology and its consequences for receiving waters: a state of the art. Adv. Water Resour. 51, 261–279. https://doi.org/10.1016/j.advwatres.2012.09.001.

Gaglio, M., Aschonitis, V.G., Mancuso, M.M., Reyes Puig, J.P., Moscoso, F., Castaldelli, G., Fano, E.A., 2017. Changes in land use and ecosystem services in tropical forest areas: a case study in Andes mountains of Ecuador. Int. J. Biodivers. Sci. Ecosyst. Serv. Manage. 13, 264–279. https://doi.org/10.1080/21513732.2017.1345980.

Gillner, S., Vogt, J., Tharang, A., Dettmann, S., Roloff, A., 2015. Role of street trees in mitigating effects of heat and drought at highly sealed urban sites. Landsc. Urban Plann. 143, 33–42. https://doi.org/10.1016/j.landurbplan.2015.06.005.

Gissi, E., Garramone, V., 2018. Learning on ecosystem services co-production in decision-making from role-playing simulation: comparative analysis from Southeast Europe. Ecosyst. Serv. https://doi.org/10.1016/j.ecoser.2018.03.025. in press.

Gissi, E., Burkhard, B., Verburg, P.H., 2015. Ecosystem services: building informed policies to orient landscape dynamics. Int. J. Biodivers. Sci. Ecosyst. Serv. Manag. 11, 185–189. https://doi.org/10.1080/21513732.2015.1071939.

Gissi, E., Gaglio, M., Reho, M., 2016. Sustainable energy potential from biomass through ecosystem services trade-off analysis: the case of the Province of Rovigo (Northern Italy). Ecosyst. Serv. 18, 1–19. https://doi.org/10.1016/j.ecoser.2016.01.004.

Gissi, E., Gaglio, M., Aschonitis, V.G., Fano, E.A., Reho, M., 2018. Soil-related ecosystem services trade-off analysis for sustainable biodiesel production. Biomass Bioenergy 114, 83–99. https://doi.org/10.1016/j.biombioe.2017.08.028.

Gómez-Baggethun, E., de Groot, R., Lomas, P.L., Montes, C., 2010. The history of ecosystem services in economic theory and practice: from early notions to markets and payment schemes. Ecol. Econ. 69, 1209–1218. https://doi.org/10.1016/j.ecolecon.2009.11.007.

Grote, R., Samson, R., Alonso, R., Amorim, J.H., Cariñanos, P., Churkina, G., Fares, S., Thiec, D.L., Niinemets, Ü., Mikkelsen, T.N., Paoletti, E., Tiwary, A., Calfapietra, C., 2016. Functional traits of urban trees: air pollution mitigation potential. Front. Ecol. Environ. 14. https://doi.org/10.1002/fee.1426.

Haaland, C., van den Bosch, C.K., 2015. Challenges and strategies for urban green-space planning in cities undergoing densification: a review. Urban For. Urban Green. 14, 760–771. https://doi.org/10.1016/j.ufug.2015.07.009.

Haase, D., Larondelle, N., Andersson, E., Artmann, M., Borgström, S., Breuste, J., Gomez-Baggethun, E., Gren, A., Hamstead, Z., Hansen, R., Kabisch, N., Kremer, P., Langemeyer, J., Rall, E.L., McPhearson, T., Pauleit, S., Qureshi, S., Schwarz, N., Voigt, A., Wurster, D., Elmqvist, T., 2014. A quantitative review of urban ecosystem service assessments: concepts, models, and implementation. Ambio 43, 413–433. https://doi.org/10.1007/s13280-014-0504-0.

Hammond, M.J., Chen, A.S., Djordjević, S., Butler, D., Mark, O., 2015. Urban flood impact assessment: a state-of-the-art review. Urban Water J. 12, 14–29. https://doi.org/10.1080/1573062X.2013.857421.

Hawkins, R.H., Ward, T., Woodward, D.E., Van Mullem, J., 2009. Curve Number Hydrology: State of the Practice. J. Hydraulics Div. ASCE publication, Reston, Viginia (USA), pp. 106. https://doi.org/10.1061/9780784410042. ISBN 978-0-7844-1004-2.

Hirschmüller, H., 2008. Stereo processing by semiglobal matching and mutual information. IEEE Trans. Pattern Anal. Mach. Intell. 30, 328–341. https://doi.org/10.1109/TPAMI.2007.1166.

Holman-Dodds, J.K., Bradley, A.A., Potter, K.W., 2003. Evaluation of hydrologic benefits of infiltration based urban storm water management. J. Am. Water Resour. Assoc. 39, 205–215. https://doi.org/10.1111/j.1752-1688.2003.tb01572.x.

Huong, H.T.L., Pathirana, A., 2013. Urbanization and climate change impacts on future urban flooding in Can Tho city, Vietnam. Hydrol. Earth Syst. Sci. 17, 379–394. https://doi.org/10.5194/hess-17-379-2013.

IPCC, 2014. In: Pachauri, R.K., Meyer, L.A. (Eds.), Climate Change 2014: Synthesis Report. Contribution of Working Groups I, II and III to the Fifth Assessment Report of the Intergovernmental Panel on Climate Change. Core Writing Team. https://doi.org/10.1017/CBO9781107415324.004.

Jim, C.Y., Chen, W.Y., 2008. Assessing the ecosystem service of air pollutant removal by urban trees in Guangzhou (China). J. Environ. Manage. 88, 665–676. https://doi.org/10.1016/j.jenvman.2007.03.035.

Kabisch, N., 2015. Ecosystem service implementation and governance challenges in urban green space planning-the case of Berlin, Germany. Land Use Policy 42, 557–567. https://doi.org/10.1016/j.landusepol.2014.09.005.

Lefsky, M.A., Cohen, W.B., Parker, G.G., Harding, D.J., 2002. Lidar remote sensing for ecosystem studies. Bioscience 52, 19–30. https://doi.org/10.1641/0006-3568(2002)052[0019:LRSFES]2.0.CO;2.

Lehmann, I., Mathey, J., Rößler, S., Bräuer, A., Goldberg, V., 2014. Urban vegetation structure types as a methodological approach for identifying ecosystem services – application to the analysis of micro-climatic effects. Ecol. Indic. 42. https://doi.org/10.1016/j.ecolind.2014.02.036.

Lim, K.J., Engel, B.A., Muthukrishnan, S., Harbor, J., 2006. Effects of initial abstraction and urbanization on estimated runoff using CN technology. J. Am. Water Resour. Assoc. 42, 629–643. https://doi.org/10.1111/j.1752-1688.2006.tb04481.x.

Ling, L., Yusop, Z., 2014. A micro focus with macro impact: exploration of initial

abstraction coefficient ratio (λ) in soil conservation curve number (CN) methodology. IOP Conference Series: Earth and Environmental Science. https://doi.org/10.1088/1755-1315/18/1/012121.

Liquete, C., Zulian, G., Delgado, I., Stips, A., Maes, J., 2013. Assessment of coastal protection as an ecosystem service in Europe. Ecol. Indic. 30, 205–217. https://doi.org/10.1016/j.ecolind.2013.02.013.

Maragno, D., 2016. Focus B: using aerial photogrammetry for urban sustainability analysis. In: Musco, F. (Ed.), Counteracting Urban Heat Island Effects in a Global Climate Change Scenario. Springer International Publishing, pp. 248–251. https://doi.org/10.1007/978-3-319-10425-6_8.

Maragno, D., Magni, F., Appiotti, F., Dalla Fontana, F., 2015. Towards the metropolitan city: adaptation strategies to climate change using new technologies. In: ECTP-CEU (Ed.), E-Governance and Spatial Planning Decision – Making. ECTP-CEU Young Planners Workshop. Avenue dD'Auderghem 63 B-1040 Brussels – Belgium, pp. 52–69.

Mason, E., Montalto, F.A., 2014. The overlooked role of New York City urban yards in mitigating and adapting to climate change. Local Environ. https://doi.org/10.1080/13549839.2014.907249.

McPhearson, T., Hamstead, Z.A., Kremer, P., 2014. Urban ecosystem services for resilience planning and management in New York City. Ambio 43, 502–515. https://doi.org/10.1007/s13280-014-0509-8.

Municipality of Dolo, 2012. Water Management Plan, D.C.C. N. 37, 26/06/2012 – Approvazione Piano Delle Acque.

Musco, F., Appiotti, F., Bianchi, I., Fontana, M.D., Gissi, E., Lucertini, G., Magni, F., Maragno, D., 2016. Planning and climate change: concepts, approaches, design. In: Musco, F. (Ed.), Counteracting Urban Heat Island Effects in a Global Climate Change Scenario. Springer International Publishing. https://doi.org/10.1007/978-3-319-10425-6. xxxvii-xlvi.

Nedkov, S., Burkhard, B., 2012. Flood regulating ecosystem services – mapping supply and demand, in the Etropole municipality, Bulgaria. Ecol. Indic. 21, 67–79. https://doi.org/10.1016/j.ecolind.2011.06.022.

Nikodinoska, N., Paletto, A., Pastorella, F., Granvik, M., Franzese, P.P., 2018. Assessing, valuing and mapping ecosystem services at city level: the case of Uppsala (Sweden). Ecol. Modell. 368, 411–424. https://doi.org/10.1016/j.ecolmodel.2017.10.013.

NRCS, 1986. Urban hydrology for small watersheds TR-55. USDA Nat. Resour. Conserv. Serv. Conserv. Eng. Div. Techol. Release 55, 164 https://doi.org/Technical Release 55.

Ojea, E., 2015. Challenges for mainstreaming ecosystem-based adaptation into the international climate agenda. Curr. Opin. Environ. Sustain. https://doi.org/10.1016/j.cosust.2015.03.006.

Panduro, T.E., Veie, K.L., 2013. Classification and valuation of urban green spaces-A hedonic house price valuation. Landsc. Urban Plann. 120, 119–128. https://doi.org/10.1016/j.landurbplan.2013.08.009.

Pappalardo, V., La Rosa, D., Campisano, A., La Greca, P., 2017. The potential of green infrastructure application in urban runoff control for land use planning: a preliminary evaluation from a southern Italy case study. Ecosyst. Serv. 26, 345–354. https://doi.org/10.1016/j.ecoser.2017.04.015.

Pitt, R., Lantrip, J., Harrison, R., Henry, C.L., Xue, D., 1999. Infiltration Through Disturbed Urban Soils and Compost-Amended Soil Effects on Runoff Quality and Quantity Project Summary. U.S. Environmental Protection Agency, Office of Research and Development, Washington, D.C [No. EPA/600/R-00/016].

Pulighe, G., Fava, F., Lupia, F., 2016. Insights and opportunities from mapping ecosystem services of urban green spaces and potentials in planning. Ecosyst. Serv. 22, 1–10. https://doi.org/10.1016/j.ecoser.2016.09.004.

Rangarajan, S., Marton, D., Montalto, F., Cheng, Z.J., Smith, G., 2015. Measuring the flow: green infrastructure grows in Brooklyn. Curr. Opin. Environ. Sustain. 17, 36–41. https://doi.org/10.1016/j.cosust.2015.09.001.

Rosenzweig, C., Solecki, W., Blake, R., Bowman, M., Faris, C., Gornitz, V., Horton, R., Jacob, K., LeBlanc, A., Leichenko, R., Linkin, M., Major, D., O'Grady, M., Patrick, L., Sussman, E., Yohe, G., Zimmerman, R., 2011. Developing coastal adaptation to climate change in the New York City infrastructure-shed: process, approach, tools, and strategies. Clim. Change 106, 93–127. https://doi.org/10.1007/s10584-010-0002-8.

Schröter, D., Cramer, W., Leemans, R., Prentice, I.C., Araújo, M.B., Arnell, N.W., Bondeau, A., Bugmann, H., Carter, T.R., Gracia, C.A., de la Vega-Leinert, A., Erhard, M., Ewert, F., Glendining, M., House, J.I., Kankaanpää, S., Klein, R.J.T., Lavorel, S., Lindner, M., Metzger, M.J., Meyer, J., Mitchell, T.D., Reginster, I., Rounsevell, M., Sabat, S., Sitch, S., Smith, B., Smith, J., Smith, P., Sykes, M.T., Thonicke, K., Thuiller, W., Tuck, G., Zaehle, S., Zierl, B., 2005. Ecosystem service supply and vulnerability to global change in Europe. Science 310, 1333–1337. https://doi.org/10.1126/science.1115233.

Shirini, B., Imaninasab, R., 2016. Performance evaluation of rubberized and SBS modified porous asphalt mixtures. Constr. Build. Mater. 107, 165–171. https://doi.org/10.1016/j.conbuildmat.2016.01.006.

Snäll, T., Lehtomäki, J., Arponen, A., Elith, J., Moilanen, A., 2016. Green infrastructure design based on spatial conservation prioritization and modeling of biodiversity features and ecosystem services. Environ. Manage. 57, 251–256. https://doi.org/10.1007/s00267-015-0613-y.

Southon, G.E., Jorgensen, A., Dunnett, N., Hoyle, H., Evans, K.L., 2017. Biodiverse perennial meadows have aesthetic value and increase residents' perceptions of site quality in urban green-space. Landsc. Urban Plann. 158, 105–118. https://doi.org/10.1016/j.landurbplan.2016.08.003.

Temmerman, S., Meire, P., Bouma, T.J., Herman, P.M.J., Ysebaert, T., De Vriend, H.J., 2013. Ecosystem-based coastal defence in the face of global change. Nature 504, 79–83. https://doi.org/10.1038/nature12859.

Tzoulas, K., Korpela, K., Venn, S., Ylipelkonen, V., Kazmierczak, A., Niemela, J., James, P., 2007. Promoting ecosystem and human health in urban areas using Green Infrastructure: a literature review. Landsc. Urban Plann. 81, 167–178. https://doi.org/10.1016/j.landurbplan.2007.02.001.

USDA, 2009. Chapter 7 hydrologic soil groups. National Engineering Handbook. (p. 5).

USDA - Soil Conservation Service, 1972. SCS national engineering handbook. Section 4, hydrology. National Engineering Handbook.

Verhagen, W., Kukkala, A.S., Moilanen, A., van Teeffelen, A.J.A., Verburg, P.H., 2017. Use of demand for and spatial flow of ecosystem services to identify priority areas. Conserv. Biol. 31, 860–871. https://doi.org/10.1111/cobi.12872.

Wang, Y., Bakker, F., De Groot, R., Wörtche, H., 2014. Effect of ecosystem services provided by urban green infrastructure on indoor environment: a literature review. Build. Environ. 31, 1–25. https://doi.org/10.1016/j.buildenv.2014.03.021.

Ward, A.D., Trimble, S.W., 2004. Environmental Hydrology. Lewis Publishers.

Wolff, S., Schulp, C.J.E., Verburg, P.H., 2015. Mapping ecosystem services demand: a review of current research and future perspectives. Ecol. Indic. 55, 159–171. https://doi.org/10.1016/j.ecolind.2015.03.016.

Yang, L., Zhang, L., Li, Y., Wu, S., 2015. Water-related ecosystem services provided by urban green space: a case study in Yixing City (China). Landsc. Urban Plann. 136, 40–51. https://doi.org/10.1016/j.landurbplan.2014.11.016.

Yao, L., Chen, L., Wei, W., Sun, R., 2015. Potential reduction in urban runoff by green spaces in Beijing: a scenario analysis. Urban For. Urban Green. 14, 300–308. https://doi.org/10.1016/j.ufug.2015.02.014.

Zhang, B., Xie, G., Zhang, C., Zhang, J., 2012. The economic benefits of rainwater-runoff reduction by urban green spaces: a case study in Beijing, China. J. Environ. Manage. 100, 65–71. https://doi.org/10.1016/j.jenvman.2012.01.015.

Zheng, H., Li, Y., Robinson, B.E., Liu, G., Ma, D., Wang, F., Lu, F., Ouyang, Z., Daily, G.C., 2016. Using ecosystem service trade-offs to inform water conservation policies and management practices. Front. Ecol. Environ. 14, 527–532. https://doi.org/10.1002/fee.1432.

Zidar, K., Bartrand, T.A., Loomis, C.H., McAfee, C.A., Geldi, J.M., Rigall, G.J., Montalto, F., 2017a. Maximizing green infrastructure in a Philadelphia neighborhood. Urban Plann. 2, 115–132. https://doi.org/10.17645/up.v2i4.1039.

Zidar, K., Belliveau-Nance, M., Cucchi, A., Denk, D., Kricun, A., O'Rourke, S., Rahman, S., Rangarajan, S., Rothstein, E., Shih, J., Montalto, F., 2017b. A framework for multifunctional green infrastructure investment in Camden, NJ. Urban Plann. 2, 56–73. https://doi.org/10.17645/up.v2i3.1038.